Research Article Vol. 15, No. 6 / 1 Jun 2024 / Biomedical Optics Express 3848
Biomedical Optics EXPRESS

# Contrast sensitivity is resilient to induced fast periodic defocus oscillations

VAHID POURREZA GHOUSHCHI, JUAN MOMPEÁN, PEDRO M. PRIETO,* AND PABLO ARTAL

*Laboratorio de Óptica, Instituto Universitario de Investigación en Óptica y Nanofísica, Universidad de Murcia, Campus de Espinardo (Edificio 34), E-30100 Murcia, Spain*
*pegrito@um.es*

**Abstract:** This study investigates the potential effects of periodic defocus oscillations on contrast sensitivity. Sinusoidal fluctuations at 5, 15, and 25 Hz, with defocus peak-to-valley values ranging from 0.15 to 3 D, were induced by means of a focus-tunable lens after calibrating its dynamic behavior. Monocular contrast sensitivity was measured on five young emmetropic subjects. The experimental data shows that contrast sensitivity loss due to defocus fluctuations is low for a wide range of frequencies and amplitudes. Only for the more severe case studied (25 Hz, ± 1.5 D) contrast threshold showed a clear increase in most subjects. Qualitative comparison of the empirical data with a simulation of modulation loss due to time integration of defocused retinal point spread functions, suggests a short integration time by the eye for defocus blur, around or even below a hundredth of a second.



## 1. Introduction

Human vision is affected by both spatial (i.e., retinal image quality) and temporal (i.e., stimulus presentation time) factors. The temporal domain has been vastly investigated [1], including visual perception in terms of image detection [2], facial expression discrimination [3], letter recognition [4], and character orientation identification [5]. These studies have shed light on the temporal limits of human vision. For instance, previous research has established that humans can detect flicker up to 500 Hz [6] and the minimum time required for letter orientation recognition is as small as 5 ms [5].

Another aspect of the temporal domain of vision is the fact that retinal image quality changes with time [7,8], mainly due to defocus [9,10] although high-order aberrations also waver [11–13]. The fluctuations due to accommodation are in the range of ±0.5 D for temporal frequencies up to 2–5 Hz, with a gradual decrease at higher temporal frequencies, although the power spectra of defocus during accommodation have non-zero components even for oscillations above 10 Hz [9]. Granting that the general consensus is that normal accommodation fluctuations probably produce too mild a blurring to affect visual performance [8], a better understanding of the eye's perception of defocus variations could help clarify this assumption.

Additionally, the use of tunable lenses for visual applications is a fast-growing field in recent years, with implications in areas such as augmented/virtual reality [14], visual diagnosis and simulation [15,16], or presbyopia correction [17], among others. Tunable lenses allow fast adjustments of defocus, typically to produce virtual objects at different distances from a fixed true object or to simulate accommodation by imaging the object of interest onto the subject's remote point. In any case, understanding how the visual system copes with these defocus changes, which can be very fast and periodic, may be critical to some present and future applications. Despite the interest and potential implications, only a limited number of studies have explored the impact of induced defocus oscillations in the human eye. In a recent study [18], the effect on visual acuity (VA) of variations of defocus in the form of sinusoidal waves with low temporal frequencies (less than 2 Hz, later increased to 4 Hz but only in combination with induced myopia [19]) was

#521340 https://doi.org/10.1364/BOE.521340
Journal © 2024 Received 8 Feb 2024; revised 8 May 2024; accepted 9 May 2024; published 20 May 2024

Biomedical Optics EXPRESS

explored and VA was found to decrease more markedly at slower temporal frequencies. Another study found that the addition of fast defocus vibrations (50 Hz) on top of an offset improved VA [20] from the static case. Finally, Ampolu et al. [21] explored the effect of defocus fluctuations associated to accommodative spasm and found that the larger the amplitude, the greater the VA loss.

In this context, this work aims to study the impact on visual function of periodic defocus fluctuations of varying amplitude and frequencies in the range between 5 and 25 Hz, too fast for the accommodative system to respond [22] but still slower than the temporal threshold for many visual tasks [1–6]. Sinusoidal fluctuations were induced by means of a tunable lens, whose dynamic operation was pre-calibrated with a 60-Hz Hartmann-Shack (HS) wavefront sensor [23]. We selected contrast sensitivity as visual performance metrics mainly because it has been shown to be sensitive to small defocus changes [24], which led us to think that it could be faster than, e.g., visual acuity (in terms of experimental data) to discern the blurring effects of dynamic defocus. To complement the experimental data, the modulation loss associated to time integration of the point-spread function (PSF) was computed for different integration intervals.

## 2. Methods

### 2.1. Experimental apparatus

A schematic view and a photograph of the optical setup are shown in Fig. 1. It is based on an open-view binocular Hartmann-Shack sensor described elsewhere [25,26]. The apparatus allows real time measurement of the ocular wavefront, in this case at an improved 60 Hz rate, while the subject has an unobstructed view of the field in front and can perform any visual task under realistic conditions. This is made possible by using a large hot mirror in front of the subject's eyes, which is transparent for visible light but redirects the invisible IR light (1050 nm wavelength) used for measurement to and from a lower stage where the HS sensor is located. A focus tunable lens with a 16 mm aperture (EL-16-40-TC-VIS-20D, Optotune Switzerland AG) was added in front of the right eye. This lens was employed to induce defocus oscillations of varying amplitudes and temporal frequencies. The left eye was occluded, and measurements were taken monocularly. The pupil monitoring camera of the apparatus was used to center the eye with respect to the tunable lens, and head movements were minimized by means of a bite bar. The stimulus generator was placed 3-m in front of the subject and consisted of a 17-inch SXGA flat monitor (UltraSharp 1704FPT, Dell Inc., USA), which was gamma calibrated using a luminance meter (LS-100, Konica Minolta, Japan). The stimuli were 1-deg, 12-cpd Gabor patches of varying contrast that were presented to the subject through the tunable lens. Lowest and highest luminance levels were 0.256 and 144.6 cd/m$^2$, respectively, with a contrast range extending from 0.005 to 0.995. A customized version of the software package to control the open-view HS [26] was developed for this experiment, including modules to configure the defocus oscillations and stimulus parameters.

### 2.2. Tunable lens dynamic calibration

The focus tunable lens used in this experiment is a liquid lens: Electrically-controlled pressure regulates the amount of liquid inside the lens, changing the shape of the encapsulating membrane and, therefore, the optical power. Liquid lenses are fast, compact, and reliable, and have a wide range of applications [16,17,27]. The model used has a 16 mm clear aperture, 7 ms response time, 40 ms settle time, –10 to +10 D optical power range, and is virtually achromatic due to the high Abbe number of the constituent fluid. Additionally, the driver offers an operation mode for inducing sinusoidal changes in defocus with selectable offset (average defocus), amplitude, and frequency, which is particularly convenient for this experiment. Placing a liquid lens in vertical has been found to produce an undesired deformation of the membrane due to gravity, that results

Biomedical Optics EXPRESS

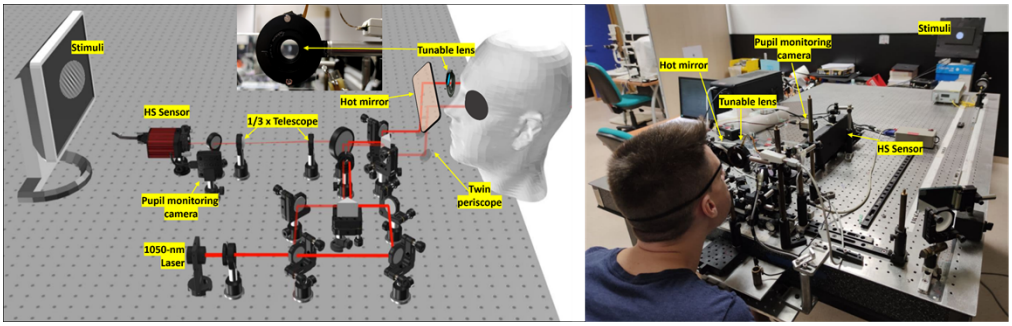


**Fig. 1.** Schematics (left) and actual implementation (right) of the optical setup based on an open-view HS sensor, with the addition of a tunable lens in front of the right eye for inducing defocus oscillations.

in a coma-like aberration. However, for the model used and the pupils considered (much smaller that the lens aperture), this comatic aberration can be neglected [28].

Static generation of optical power was calibrated by measuring with the HS sensor the defocus induced for a range of input currents [28]. However, when this calibration was used to set the periodic fluctuations of defocus, the lens was found to underachieve, especially for higher frequencies. Consequently, we measured the dynamics of the defocus fluctuations for a mesh of amplitudes and oscillating frequencies. Fourier analysis showed correct frequency production in all cases but reduced defocus amplitude by a factor proportional to the frequency. This information was used to increase the programmed amplitudes to achieve the desired oscillations for each frequency. Peak-to-valley (PtoV) values mentioned henceforth are actual ones, as opposed to programmed values. More details on the dynamic calibration procedure can be found elsewhere [29], including an analysis of the effect of defocus offset (i.e., mean value), which was not relevant for this work as all oscillations were around 0 D.

### 2.3. Subjects

Five young emmetropic subjects (three male and two female, age = 26.6 ± 4.0) with a mean refraction of –0.15 ± 0.24 D and a cylinder between 0 and –0.25 D participated in the experiment. Objective and subjective refraction was measured with an adaptive optics visual simulator (VAO, Voptica SL, Murcia, Spain). None of the individuals had visual impairments or prior surgery and all of them reached 20/20 VA or better. Before conducting the measurements, the subjects were informed about the experimental procedure, purpose, and potential dangers and their written consent was obtained. The study follows the tenets of the Helsinki Declaration and the ethical guidelines of the University of Murcia.

### 2.4. Experimental procedure

**Table 1. Mean pupil radius ± standard deviation throughout the experiment**

| Subject | S1 | S2 | S3 | S4 | S5 |
|---|---|---|---|---|---|
| Pupil radius (mm) | 3.29 ± 0.34 | 3.02 ± 0.45 | 3.16 ± 0.22 | 3.05 ± 0.38 | 3.86 ± 0.27 |

The experiment took place in a dark room. No cycloplegic was used to paralyze accommodation because, according to the literature, the accommodative system cannot follow defocus oscillations faster than 2 Hz [22], and the lowest frequency considered, 5 Hz, was beyond that threshold. To further confirm this assumption defocus was measured through the tunable lens while the experiment was performed, and no attenuation of the defocus fluctuations was observed (see

Biomedical Optics EXPRESS

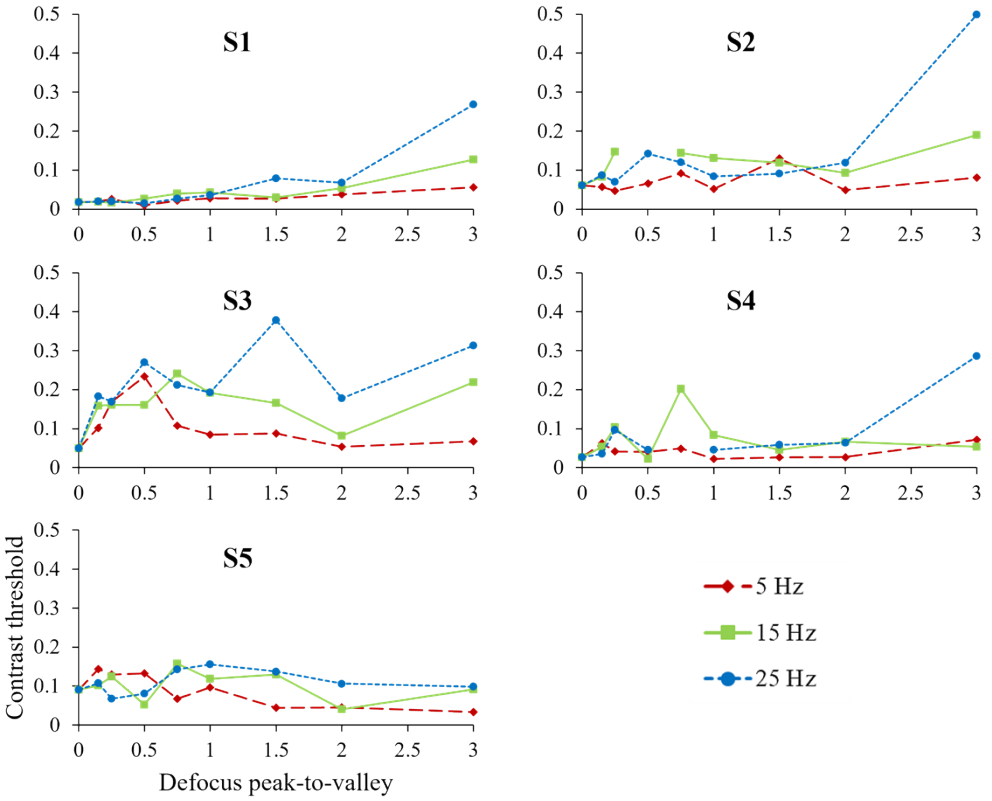


**Fig. 2.** Contrast threshold as a function of defocus PtoV for 12-cpd 1-deg Gabor gratings seen through sinusoidal defocus oscillations induced by a tunable lens. Each graph corresponds to a subject (S1 to S5). Each color represents a temporal frequency of fluctuation (see legend).

Supplement 1 for examples of measured defocus for each subject). Additionally, pupil size was monitored throughout the experiment. Mean values and standard deviations are shown in Table 1. The visual stimulus was a 12-cpd Gabor patch subtending 1 degree of visual field. This frequency was selected as a convenient trade-off, as lower frequencies are less sensitive to defocus (static and dynamic, see Supplement 1 for simulations) and higher frequencies have low contrast thresholds even at best focus. The stripes were tilted 10 degrees from the vertical in either direction. Measurements were conducted in monocular vision with the right eye in all cases. Temporal frequencies of the applied sinusoidal waves were 5, 15, and 25 Hz, with PtoV values ranging from 0.15 to 3 D.

For each experimental condition, a preliminary estimate of the contrast threshold was obtained by the adjustment method, which served as the starting point for the forced-choice method [30]. The adjustment protocol began with a high contrast value and the subject used the up and down arrow keys to determine their lowest visible contrast [31]. In the forced-choice phase, 5 contrast values were employed, in a geometric progression around the adjustment estimate for each oscillation case: 2×, 1×, 1/2, 1/4, and 1/8. Before proceeding to the measurement round, the subject was shown the series of contrast values to check that they encompassed the actual contrast threshold. If the subject was able to see all or none of them, the values were halved or doubled, respectively. There were 10 trials per oscillation case and contrast value, evenly divided in 10 series with rest breaks between them. Each series was randomized in blocks across temporal frequencies and then each block across contrast and PtoV values. During each presentation,

Biomedical Optics EXPRESS

the subject was required to guess the tilt direction of the stripes and answer with the left and right arrow keys. Each Gabor patch was displayed for 2 seconds but an earlier answer by the subject stopped the presentation and triggered the next one. Very rarely a subject took longer than this time to take a decision (even if it was deciding to guess an answer when unable to see the stimulus), meaning that presentation time was not really an issue for this experiment. For each oscillation condition, the success rate as a function of contrast was adjusted to a sigmoid function and the contrast threshold was taken at the 75% success level.

## 3. Experimental results

Pupil size was routinely measured through the experiment. Table 1 shows the mean pupil radius in mm for each subject together with the standard deviation.

Individual contrast thresholds as a function of defocus PtoV are depicted in Fig. 2. Except for a few outliers for subject S3 and one for subject S4, the subjects were able to detect the correct direction of the Gabor patch with contrast as low as 0.2 for PtoV values up to 2 D at all temporal frequencies. Only for 3 D PtoV and the fastest oscillation rate did the threshold become clearly worse for most subjects.

Figure 3 summarizes the results: it shows mean contrast threshold across subjects as a function of defocus PtoV at each frequency. Error bars represent standard deviation across subjects. The mean contrast threshold at 5 Hz can be seen to remain fairly flat as the amplitude of the oscillation increases. For 15 Hz, the mean contrast threshold exhibits moderate deterioration and variability across different defocus powers. At 25 Hz, contrast degradation was more noticeable, with the most significant loss occurring at 3 D PtoV defocus.

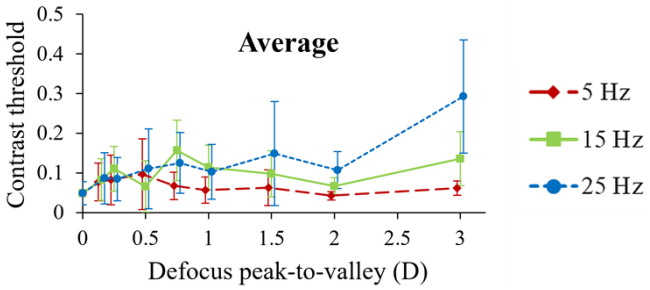


**Fig. 3.** Mean 12-cpd contrast threshold for 5, 15, and 25 Hz defocus oscillations as a function of PtoV, obtained by averaging across subjects the data points in Fig. 2. Error bars represent the standard deviation across subjects. Symbols for different frequencies were slightly shifted in horizontal direction to aid visibility of the error bars.

## 4. Simulation

Defocus fluctuations produce a temporal evolution of the PSF. At the fast temporal frequencies and with the long presentation time considered in this work, the instantaneous PSF becomes increasingly and decreasingly blurred but goes through a best focused version at periodic intervals related to the oscillation frequency. However, the eye cannot possibly follow this series of instantaneous PSFs, as some kind of integration time (in the photoreceptors and/or other levels of the visual system) must be at work. Therefore, the eye is expected to always experience some level of blurring, since the instantaneous best focus image would be combined with some other defocused images in the integration time. Assuming that the irradiance is simply accumulated point by point during this hypothetical integration time, the apparent PSF would be the average of the sequence of defocused PSFs over that period and the loss in contrast produced by the ensuing

Biomedical Optics EXPRESS

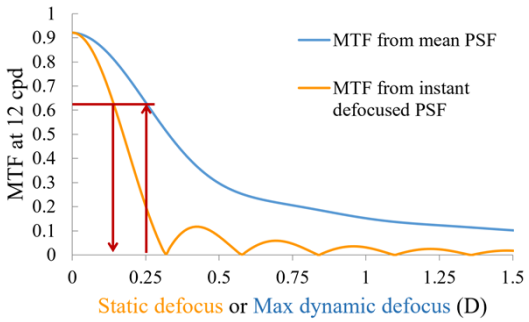


**Fig. 4.** MTF at 12 cpd for static and dynamic (ramp) defocus. For the static case (orange line), the x-axis represents the amount of defocus. For the dynamic case (blue line), the x-axis represents the Max defocus in the sweep (the MTF comes from the average PSF in the range [-Max, +Max] D). Red lines illustrate the protocol for obtaining data points for Fig. 5.

blurring could be determined from the (combined) MTF obtained from this averaged PSF. But it is important to note that MTF computing is not a linear process, which means that the combined MTF cannot be calculated by averaging the instantaneous MTFs. On the contrary, the complex optical transfer function (OTF) is the Fourier transform of the PSF, which is a linear operation. Therefore, the combined MTF can be obtained as the absolute value of the mean OTF.

With all this in mind, the aim of this simulation was to calculate the MTF expressing the loss in contrast associated to the mean blur caused by a defocus variation in an integration time. This can be done either by averaging the defocused PSFs and Fourier-transforming the result or by averaging the corresponding series of OTFs, which was the option that we used. We considered an integration time containing the 0-defocus case, which would be the best "frame" available to the eye (the rest in the sequence should be more heavily blurred). Furthermore, we did defocus averaging centered around best focus, that is, with the same amount of positive and negative values and with the minimal possible extreme defocus in absolute value. To do this, we calculated the instantaneous defocus values in $10^{-4}$-sec steps across integration times of varying lengths, always centered around the 0-D point. But instead of calculating the series of PSFs and the OTFs for each ensemble of exact defocus values, which would involve a massive number of computations, these defocus values were rounded to the hundredth of a diopter and the associated OTFs were taken from a set precalculated for defocus values in the range between 0 D and 1.5 D in 0.01 D steps, were we took advantage of the fact that negative and positive pure defocus produces exactly the same PSF. The rounding errors in defocus were so small as to produce virtually no effect in the PSF. Additional parameters for the calculations were a 6-mm pupil diameter sampled in 128 pixels, a 256-pixel Fourier transform window, and a wavelength of 545 nm.

To give a first insight on the blurring effects of dynamic defocus, we considered the case of a defocus ramp around best focus, i.e., a linear variation between -Max and + Max (PtoV = 2·Max), where Max represents the maximum defocus value. The orange curve in Fig. 4 corresponds to the 12-cpd MTF for fixed defocus values (x-axis). Its behavior is well-known: It initially drops due to the blurring caused by the widening PSF and then goes through a series of null values with phase reversals (alternating sign portions of the OTF, which are not apparent in the curve, as it represents an absolute value) interspersed. The blue line, on the other hand, is the MTF obtained from averaging the 12-cpd OTFs in a defocus range around 0 D, with the x-axis representing the Max value. There are no null values or phase reversals, and the drop in the MTF is less marked. In fact, for defocus values below the first phase reversal for the static case, there is a constant scale factor between the curves of 0.53, as can be seen in Fig. 5, were the static defocus (y-axis)

Biomedical Optics EXPRESS

and dynamic defocus (x-axis) producing the same 12-cpd MTF value are related. The data points in this figure were obtained from Fig. 4, by pairing the positions where the orange curve and blue curves have the same height (the procedure is illustrated in Fig. 4 for 0.25 D of dynamic defocus). This means that averaging defocus in a range across best focus apparently has a blurring effect similar to around half its maximum value (a quarter of PtoV) of static defocus. This factor seems to be consistent across spatial scales, since repeating the analysis for lower and higher spatial frequencies produced results very similar to Fig. 5 (see Supplement 1), for defocus values below the first null in each case.

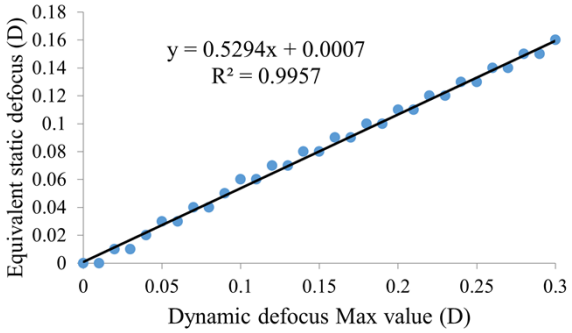


**Fig. 5.** Equivalence in blurring effects between static and dynamic (ramp) defocus: According to Fig. 4, a linear defocus scan with a Max value in the x-axis (range [-Max, +Max] D) produces the same drop in the 12-cpd MTF as the equivalent amount of static defocus in the y-axis.

The next step in the simulation consisted of calculating the 12-cpd MTFs for sinudoidal defocus oscillations with the same temporal frequencies and amplitudes considered in the experiment, combined with a range of integration times from 5 to 30 ms. However, direct comparison of these values with the experimental threshold values is not straightforward. Instead, we calculated the "modulation loss" as the ratio between the diffraction-limited MTF at 12 cpd and the calculated MTF values at the same spatial frequency. These ratios, then, would represent how many times lower than the ideal case would the MTF affected by defocus oscillations be, which could be expected to produce a similar increase in the contrast threshold.

Results of simulated modulation loss for the experimental conditions are displayed in Fig. 6, panels (a) to (e). The scale of the y-axis has been selected to have a proportionality for modulation loss similar to the scales in Figs. 2 and 3 have for contrast threshold, thus enabling qualitative comparison between them. For very short integration times and/or slow fluctuations, modulation loss is low because the PSF does not have time to change. As the integration time and/or frequency increase, the blurring effect becomes more noticeable and the modulation loss becomes apparent. For comparison purposes, panel (f) presents the modulation loss when the whole defocus range is integrated. This would be approximately equivalent to averaging the blur over an extended period of time, larger than a cycle, and would represent the upper limit of modulation loss.

Biomedical Optics EXPRESS

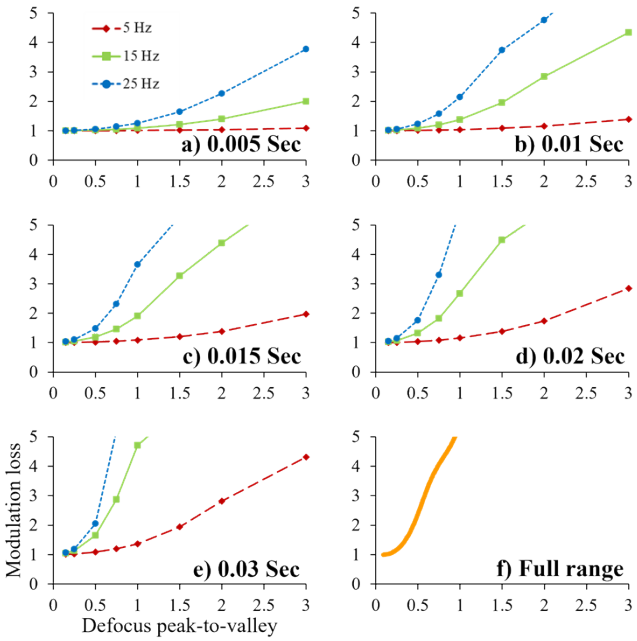


**Fig. 6.** Panels (a) to (e): Modulation loss (diffraction-limited MTF divided by integrated MTF) at 12 cpd, caused by defocus oscillations at 5 Hz (red), 15 Hz (green), and 25 Hz (blue), as a function of PtoV for different integration times. Panel (f): Modulation loss caused by whole range integration. Pupil diameter = 6 mm in all cases.

## 5. Discussion

The purpose of this study is to shed light on how the visual system processes unstable, defocus-blurred images and to provide more information on the defocus perception mechanism in the eye. Additionally, the induced defocus changes by focus tunable lenses have recently had applications in wearable optoelectronic spectacles for correcting presbyopia [17] and instruments for visual simulation [16].

To the best of our knowledge, this is the first work investigating the potentially deleterious effect of fast defocus fluctuations around emmetropia on contrast sensitivity. Numerous studies have investigated the temporal limits of the visual system but most of them explored this aspect of visual perception with static and/or fixed defocus stimuli. The small number of studies that applied defocus oscillations are conceptually different from the present work, starting with the fact that all of them measured VA instead of contrast sensitivity. Bartuzel et al [20] induced fast vibrations in defocus but they did it around a defocus, as they were interested in the potentially beneficial effect of fluctuations for ametropic subjects. On the contrary, Umemoto and Hirata induced 1-Hz defocus fluctuations but they studied the accommodative response and not visual quality [32]. Ampolu et al [21] studied the effect of simulating the broadband fluctuations of defocus (associated to accommodative spasm) and therefore could not study the effect of different temporal frequencies and varying amplitudes.

The works in the literature with more similarities with ours are those by Goswami and Bharadwaj. They analyzed the effect on VA of periodic defocus relatively slow variations, initially up to 2 Hz [18] and later 4 Hz (with induced myopia) [19], and developed a model based on the 0-crossing probability in a stimulus presentation epoch, which increases (hence improving performance) for faster fluctuations. Their conclusions were that larger PtoV and slower defocus oscillations had a more deleterious effect on visual quality. While the behavior with PtoV is very

Biomedical Optics EXPRESS

intuitive and in perfect agreement with our experimental and simulated data, there appears to be a conflict in our conclusions for que oscillation frequency. This is most probably due to the fact that we are considering a very different paradigm. Apart from using contrast sensitivity instead of visual acuity, which can have some implications in our results, the faster frequencies and long presentation times mean that the 0-crossing probability is always 1 in our case, and the relevant parameter is the range of defocus averaged in an integration time, which increases the perceived blur for higher frequencies.

For fast defocus fluctuations, the mechanism of signal integration is critical. Long-term integration is ruled out by the experimental results, since it would produce, for all temporal frequencies, curves similar to that shown in panel (f) of Fig. 6. Although numerical comparison between experimental and simulated loss of modulation is unadvisable considering the small number of subjects, qualitative assessment of Figs. 3 and 6 suggests an integration time for defocus probably below one-hundredth of a second.

As a matter of fact, the integration time could be smaller, considering that the simulation was always performed around 0 D. This is the best-case scenario as it would mean that the visual system performs a rolling sum of signal (instantaneous old data is discarded as instantaneous new data is received). If time integration by the eye is sequential (i.e., in a frame-by-frame fashion), synchronicity between defocus oscillations and visual temporal sampling could play a role and loss of modulation for each integration time could be worse than shown in Fig. 6. Actually, here we could find a secondary advantage of using contrast sensitivity instead of visual acuity. The latter involves small targets and is more related to single cone (or small group) time integration, which is probably sequential instead of rolling-like. Conversely, contrast sensitivity targets are relatively large, and many photoreceptors are at work for their detection. Unless there was a global trigger for the whole visual system (of which there is no evidence, to our knowledge) to synchronize all the integration sequences, they could be randomly distributed, and the combined effect could be more similar to a rolling integration.

Defocus can be understood as a low order aberration and its interaction with the subject's high order aberrations is not straightforward. However, all the subjects in this study had normal high order aberrations and, although they would affect the PSF around best focus, it is unlikely that they would change the eye's perception of blurring when large defocus values are involved. Considering this and the fact that taking into account the individual high order aberrations of each subject would complicate the computations (in fact, it would require one simulation per subject), we performed the simulations only considering pure defocus.

As for the practical implications of this work, accommodation microfluctuations do not exceed the temporal frequencies studied here and the typical amplitudes, for normal eyes, are well below 1 D [7,8]. The eye's relative immunity to defocus variations, found in this work, supports the common assumption that typical microfluctuations should not greatly affect visual performance. On the other hand, our results can be considered good news for the visual applications of tunable lenses involving multiple plane focusing since the visual system seems to be relatively immune to fast changes of defocus provided that the "object" is in focus for a short period of time.

## 6. Conclusion

Contrast sensitivity was measured at 12 cpd in young emmetropes under the influence of fast oscillations in defocus with different amplitudes and frequencies. The experimental results showed very limited effect in most cases. Only for fast, large variations of defocus (25 Hz, ± 1.5 D) was a clear reduction in contrast sensitivity found. A quantitative model was developed for predicting the deterioration in retinal image quality due to periodic defocus fluctuations as a function of integration time. For the amplitudes and frequencies of oscillation used in the experiment, the extended-time MTF at 12 cpd was calculated from the average OTF. Qualitative

Biomedical Optics EXPRESS

comparison between experimental results and simulated data suggests that the eye may be integrating defocus in the hundred-Hz range.

**Funding.** Fundación Séneca (19897/GERM/15); Agencia Estatal de Investigación (AEI/10.13039/501100011033, PID2019-105684RB-I00); Horizon 2020 Framework Programme (675137).

**Disclosures.** The authors declare no conflicts of interest.

**Data availability.** Data underlying the results presented in this paper are not publicly available at this time but may be obtained from the authors upon reasonable request.

**Supplemental document.** See Supplement 1 for supporting content.

## References

1. P. Fraisse, "Perception and estimation of time," Annu. Rev. Psychol. **35**(1), 1–37 (1984).
2. M. C. Potter, B. Wyble, C. E. Hagmann, *et al.*, "Detecting meaning in RSVP at 13 ms per picture," Atten. Percept. Psychophys. **76**(2), 270–279 (2014).
3. M. Milders, A. Sahraie, and S. Logan, "Minimum presentation time for masked facial expression discrimination," Emotion **22**(1), 63–82 (2008).
4. C. Bundesen and L. Harms, "Single-letter recognition as a function of exposure duration," Psychol. Res. **62**(4), 275–279 (1999).
5. L. Sawides, A. Gambín-Regadera, A. de Castro, *et al.*, "High speed visual stimuli generator to estimate the minimum presentation time required for an orientation discrimination task," Biomed. Opt. Express **9**(6), 2640–2647 (2018).
6. J. Davis, Y. H. Hsieh, and H. C. Lee, "Humans perceive flicker artifacts at 500 Hz," Sci. Rep. **5**(1), 7861 (2015).
7. G. Walsh and W. N. Charman, "Visual sensitivity to temporal change in focus and its relevance to the accommodation response," Vision Res. **28**(11), 1207–1221 (1988).
8. W. N. Charman and G. Heron, "Microfluctuations in accommodation: an update on their characteristics and possible role," Ophthalmic Physiol. Opt. **35**(5), 476–499 (2015).
9. A. W. Lohmann and D. P. Paris, "Influence of longitudinal vibrations on image quality," Appl. Opt. **4**(4), 393–397 (1965).
10. S. R. Bharadwaj, "Accommodation mechanisms," in *Handbook of Visual Optics, Volume One*, P. Artal, ed. (CRC Press, 2017).
11. H. Hofer, P. Artal, B. Singer, *et al.*, "Dynamics of the eye's wave aberration," J. Opt. Soc. Am. A **18**(3), 497–506 (2001).
12. A. Mira-Agudelo, L. Lundström, and P. Artal, "Temporal dynamics of ocular aberrations: monocular vs binocular vision," Ophthalmic Physiol. Opt. **29**(3), 256–263 (2009).
13. S. Manzanera and P. Artal, "Stability of the retinal image under normal viewing conditions and the implications for neural adaptation," Sci. Rep. **14**(1), 2280 (2024).
14. N. Padmanaban, R. Konrad, E. A. Cooper, *et al.*, "Optimizing VR for all users through adaptive focus displays," in ACM SIGGRAPH 2017 Talks (SIGGRAPH '17) (2017), Article 77.
15. S. R. Soomro, S. Sager, A. M. Paniagua-Diaz, *et al.*, "Head-mounted adaptive optics visual simulator," Biomed. Opt. Express **15**(2), 608–623 (2024).
16. C. Dorronsoro, E. Gambra, L. Sawides, *et al.*, "Experimental validations of a tunable-lens-based visual demonstrator of multifocal corrections," Biomed. Opt. Express **9**(12), 6302–6317 (2018).
17. J. Mompeán, J. L. Aragón, and P. Artal, "Portable device for presbyopia correction with optoelectronic lenses driven by pupil response," Sci. Rep. **10**(1), 20293 (2020).
18. S. Goswami and S. R. Bharadwaj, "Impact of temporal fluctuations in optical defocus on visual acuity: Empirical results and modeling outcomes," J. Vision **23**(3), 14 (2023).
19. S. Goswami and S. R. Bharadwaj, "Temporal fluctuations in defocus may reverse the acuity loss encountered with induced refractive errors," J. Opt. Soc. Am. A **40**(11), 2008–2018 (2023).
20. M. M. Bartuzel, D. R. Iskander, I. Marín-Franch, *et al.*, "Defocus vibrations in optical systems-considerations in reference to the human eye," J. Opt. Soc. Am. A **36**(3), 464–470 (2019).
21. N. Ampolu, D. Yarravarapu, P. Satgunam, *et al.*, "Impact of induced pseudomyopia and refractive fluctuations of accommodative spasm on visual acuity," Clin. Exp. Optom. **106**(8), 876–882 (2023).
22. V. Rodriguez-Lopez, A. Hernandez-Poyatos, and C. Dorronsoro, "Defocus flicker of chromatic stimuli deactivates accommodation," Biomed. Opt. Express **14**(7), 3671–3688 (2023).
23. V. P. Ghoushchi, J. Mompeán, P. M. Prieto, *et al.*, "Effect of periodic defocus oscillations on contrast sensitivity," Invest. Ophthalmol. Vis. Sci. **63**, 3060s–F0532 (2022).
24. H. Radhakrishnan, S. Pardhan, R. I. Calver, *et al.*, "Effect of positive and negative defocus on contrast sensitivity in myopes and non-myopes," Vision Res. **44**(16), 1869–1878 (2004).
25. E. Chirre, P. Prieto, and P. Artal, "Dynamics of the near response under natural viewing conditions with an open-view sensor," Biomed. Opt. Express **6**(10), 4200–4211 (2015).
26. V. P. Ghoushchi, J. Mompeán, P. M. Prieto, *et al.*, "Binocular dynamics of accommodation, convergence, and pupil size in myopes," Biomed. Opt. Express **12**(6), 3282–3295 (2021).

Biomedical Optics EXPRESS

27. L. Chen, M. Ghilardi, J. J. C. Busfield, *et al.*, "Electrically tunable lenses: a review," Front Robot AI **8**, 678046 (2021).
28. N. Suchkov, E. J. Fernández, and P. Artal, "Wide-range adaptive optics visual simulator with a tunable lens," J. Opt. Soc. Am. A **36**(5), 722–730 (2019).
29. V. P. Ghoushchi, "Study of accommodation dynamics and defocus fluctuations in the human eye," Doctoral Thesis, Universidad de Murcia (2023).
30. C. C. Wier, W. Jesteadt, and D. M. Green, "Comparison of method-of-adjustment and forced-choice procedures in frequency discrimination," Percept. Psychophys. **19**(1), 75–79 (1976).
31. J. Richman, G. L. Spaeth, and B. Wirostko, "Contrast sensitivity basics and a critique of currently available tests," J. Cataract Refract. Surg. **39**(7), 1100–1106 (2013).
32. S. Umemoto and Y. Hirata, "Temporal changes in accommodative responses to periodic visual motion," Vision Res. **191**, 107969 (2022).